Proceedings of the ASME 2020 Conference on Smart Materials, Adaptive Structures and Intelligent Systems
SMASIS2020
September 15, 2020, Virtual, Online

SMASIS2020-2331

IMPACT OF INCLUDING ELECTRONICS DESIGN ON DESIGN OF INTELLIGENT STRUCTURES: APPLICATIONS TO MULTIFUNCTIONAL STRUCTURES FOR ATTITUDE CONTROL (MSAC)

Vedant
University of Illinois at Urbana-Champaign
Aerospace Engineering
Urbana, IL 61801
Email: vedant2@illinois.edu

James T. Allison
University of Illinois at Urbana-Champaign
Industrial & Enterprise Systems Engineering
Aerospace Engineering
Urbana, IL 61801
Email: jtalliso@illinois.edu

ABSTRACT

Multifunctional Structures for Attitude Control (MSAC) is a new spacecraft attitude control system that utilizes deployable panels as multifunctional intelligent structures to provide both fine pointing and large slew attitude control. Previous studies introduced MSAC design and operation concepts, simulation-based design studies, and Hardware-in-the-Loop (HIL) validation of a simplified prototype. In this article, we expand the scope of design studies to include individual compliant piezoelectric actuators and associated power electronics. This advance is a step toward high-fidelity MSAC system operation, and reveals new design insights for further performance enhancement. Actuators are designed using pseudo rigid body dynamic models (PRBDMs), and are validated for steady-state and step responses against Finite Element Analysis. The drive electronics model consists of a few distinct topologies that will be used to evaluate system performance for given mechanical and control system designs. Subsequently, a high-fidelity multiphysics multibody MSAC system model, based on the validated compliant actuators and drive electronics, is developed to support implementation of MSAC Control Co-design optimization studies. This model will be used to demonstrate the impact of including the power electronics design in the Optimal Control Co-Design domain. The different control trajectories are compared for slew rates and the vibrational jitter introduced to the satellite. The results from this work will be used to realize closed-loop control trajectories that have minimal jitter introduction while providing high slew rates.

1 Introduction

Spacecraft attitude control is the process of orienting a satellite towards different points of interest in space, precisely and accurately. These functionalities of the attitude control system are generally required for the proper functioning of both the spacecraft and the science payload. The performance of an attitude control system can be measured using several metrics; two metrics that are important for many space missions include pointing accuracy and pointing stability [1]. Spacecraft with optical payloads have traditionally demanded the highest levels of pointing accuracy, up to the nano-radian (milli-arc-second) scale [2]. Multiple new space telescopes are being designed with unprecedented levels of required pointing accuracy [3–5], motivating the development of new ACS technologies with enhanced accuracy (while maintaining or improving reliability).

Spacecraft attitude control has been provided conventionally by several technologies, including reaction thrusters, magnetic torque coils, and momentum management devices; Reaction Wheel Assemblies (RWAs), Control Moment Gyroscopes (CMGs), and nutation dampers are examples of moment management devices [7]. A key benefit of momentum management devices is that they produce attitude changes by temporarily altering the distribution of angular momentum between devices and the rest of the spacecraft, without expending fuel to produce any external torques. Despite the flight heritage of RWAs and CMGs, several mission lifespans have been shortened due to the common failure modes common to RWA and CMG based Attitude Control System (ACS), resulting in an inability to provide

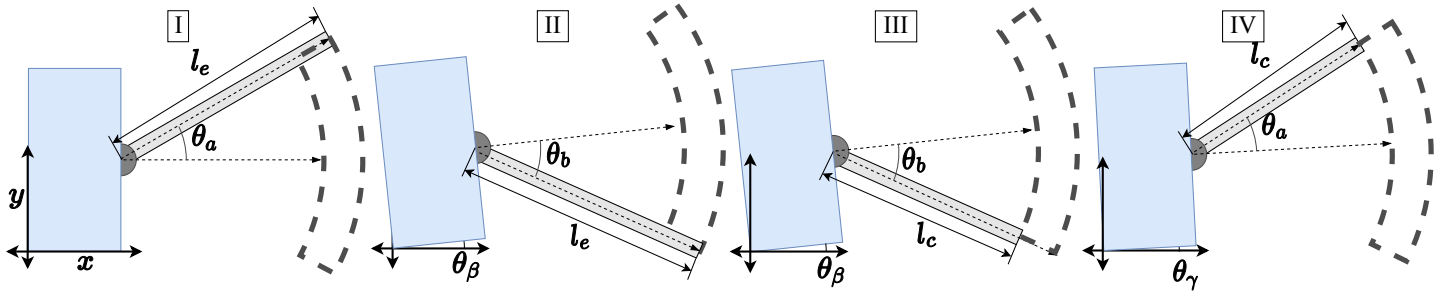

FIGURE 1: MSAC system demonstration with the non-holonomic trajectories. The reachable space for the appendage/deployable panel can be seen as the dashed yellow annulus ring sector. This control trajectory has been discussed and analyzed in more detail in Ref [6].

the pointing required by the science payload [8].

Recent spacecraft with higher pointing accuracy and stability demands (sub-arc-second) utilize RWAs or CMGs for arbitrarily-large attitude control maneuvers, coupled with vibration isolation systems, to achieve the required performance [9]. The pointing accuracy, stability, and reliability required from ACS systems for future missions motivate the investigation of fundamentally new ACS strategies with potential for quieter and more reliable operation.

The Strain-Actuated Solar Array (SASA) ACS was developed as a joint effort between the University of Illinois and NASA JPL and NASA Ames to replace massive passive vibration isolation systems with active jitter cancellation using the deployed solar-panels as multifunctional structures. These panels provide precise, but limited (small angle), attitude control in addition to their primary functions. The SASA system has demonstrated cancellation of mechanical vibration (jitter), and producing small slew maneuvers that hold a pose for short time periods [10, 11].

A novel extension of the original SASA system, known as Multifunctional Structures for Attitude Control (MSAC), was introduced recently [6, 12, 13]. MSAC augments the capabilities of the SASA system with the capability of producing arbitrarily-large slews about all rotation axes. This new functionality is achieved through mechanical and control system design modifications that support non-holonomic trajectories required for unlimited slew angle magnitudes. These trajectories have some similarities with older concepts that also use variable mass moments of inertia (VMOI), but the embodiment is fundamentally different. Earlier efforts relied on mechanical designs with sliding mode contacts [14, 15], whereas MSAC utilizes monolithic structures, eliminating a key failure mode that is inherent not only to the earlier VMOI concepts, but also to current RWA and CMG technologies.

The article first summarizes the current state-of-art of the MSAC concept and the development and validation of the concept using conventional methods. Then, a new detailed design process is explained that utilizes Pseudo-Rigid Body Models (PRBMs) developed for compliant mechanisms to design compliant actuators [16] without requiring expensive Finite Element Analysis (FEA). The lumped MSAC prototype that has been realized [12] had a strong two-way coupling between the mechanical design and the control trajectories that enable the large slews. Such classes of problems are known as Control Co-Design (CCD) problems [17]. Next, the obtained design is validated using finite element analysis (FEA) for the predicted performance. After validating the mechanical response of the actuator, the PRBM model along with the control design is realized in Simulink. The Simulink model is then utilized to obtain system performance for trivial control trajectories. The paper concludes with increasing the fidelity of the Simulink model to include the drive electronics designed to realize designed the control trajectories, and the difference in energy consumed for different electronic designs are presented.

2 State-of-the-Art

The MSAC system was discovered when the SASA concept was realized in a 3D physics engine and the Pseudo Rigid Body Dynamic Models (PRBDMs) representing the system exhibited a secular attitude maneuver with random inputs. The MSAC system utilizes existing deployable structures/appendages (such as solar arrays or radiators) as multifunctional devices. This multi-role use of the solar panels extends their utility at a low mass penalty, while increasing spacecraft ACS reliability.

In a previous study, the principle of operation of the MSAC system was introduced in detail and the initial designs for compliant actuators that enable the MSAC concept were introduced [6]. The utilization of transverse oscillations of the deployable panels combined with moment of inertia (MOI) reconfigurations, enables secular attitude slews. Both oscillations and reconfigurations are achieved by exercising the same set of distributed actuators. Strategic adjustments to MOI between transverse oscillations produce a secular change in attitude, one such simplified trajectory is demonstrated in Fig. 1. One mechanism for changing MOI is to induce longitudinal strains, increasing or decreasing the MOI about the vehicle axis of rotation. To illustrate one possible instantiation of the MSAC concept, the two constituent

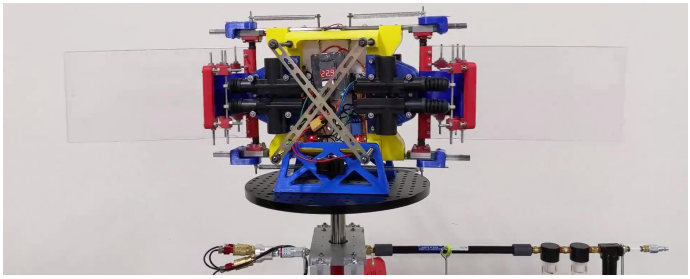

FIGURE 2: Current Technology Readiness Level (TRL) of MSAC concept: Hardware-in-the-loop (HIL) validation of low fidelity MSAC prototype using a one degree of freedom roller bearing (TRL 3).

phases are illustrated using a single axis of rotation MSAC system as follows:

1. Strain deployable structures for jitter control or for producing small slew maneuvers in the transverse panel direction. This is illustrated in Fig. 1, Phase I to Phase II or Phase III to Phase IV.
2. Strain deployable structures to alter inertial properties, seen in Fig. 1, straining from Phase II to Phase III or Phase IV to Phase I.

In fig. 1 Phase IV, it can be seen that the satellite body has rotated by a small angle θ_γ, while the panels have been reset back to the same relative orientation with respect to the spacecraft as in Phase I (θ_a).

Using the simplified system models, an estimate of performance metrics for the slew rates were derived, utilizing conservation of angular momentum, obtaining Eqn. (2)

$$I_{\text{sat}}(\theta_\gamma) = (I_e - I_c)(\theta_a - \theta_b), \tag{1}$$

$$\theta_\gamma = \frac{(I_e - I_c)}{I_{\text{sat}}}(\theta_a - \theta_b). \tag{2}$$

The average angular velocity of the attitude maneuver can be approximated using the following linear approximation:

$$\omega_\gamma \approx \frac{\theta_\gamma}{\Delta t} = \frac{(I_e - I_c)(\theta_a - \theta_b)}{I_{\text{sat}}\Delta t}, \tag{3}$$

where $\Delta t = t_{bc} + t_{be} + t_e + t_c$ is the time required to perform one complete cycle (Phase I through Phase IV), as illustrated in Fig. 1.

Next, a simplified prototype utilizing linear solenoid actuators and rapid prototype parts to perform a Hardware-in-the-Loop (HIL) test for the MSAC concept. After the initial validation of the MSAC concept in physics simulations, the MSAC concept was realized using inexpensive lumped electrical actuators (solenoids) and 3D-printed parts. The linear solenoid actuators were used with mechanisms that mimicked the lumped DOFs of the PRBDM model from Fig. 1. The realized prototype, depicted in Fig. 2, was tested for attitude slews on a single

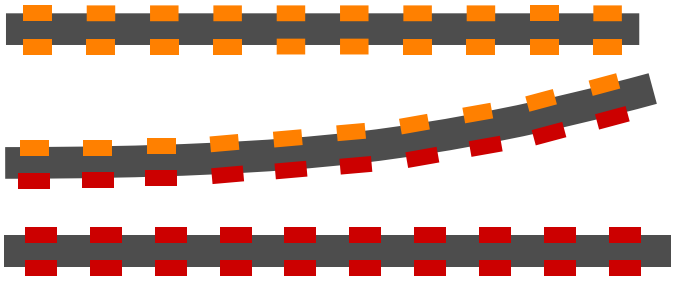

FIGURE 3: Illustration of distributed strain actuators used to produce the contraction, bending, and extension deformations. Strain actuators (e.g., piezoelectric patches, electromagnetic coils, etc.) are depicted using small boxes attached to the deployable structure body. Actuators undergoing extension are shown in red, and those undergoing contraction are shown in orange.

DOF (vertical axis) roller bearing testbed. The results from this provided hardware validation of the concept, albeit with discrete actuators which were actuated with relays, and thus only had binary bang-bang control capability. These limitations constrained the panel actuation frequency to be close to the first natural harmonic, and thereby constrained the attitude slew rate and impacted system jitter.

3 Compliant actuator design

With the recent validation of the MSAC concept and reaching a NASA Technology Readiness Level (TRL) of 3 [12], the next task was to design and realize compliant actuators that can enable high fidelity MSAC capability, as seen in Fig. 3. To realize non sliding mode based actuation, capable of producing depicted in Fig. 3, an example actuator mechanism utilizing piezoelectric elements was proposed in Ref. [6]. The actuator realized in this study was based on the previously proposed compliant actuator design, modified for ease of manufacturability. The actuator consists of piezoelectric elements embedded in a metallic bar. The bar is strained in the longitudinal direction by actuating the piezoelectric elements. Some types of piezoelectric actuators can achieve both extension and contraction via different modes of actuation. The first task is to realize the lever-based actuator presented in Ref. [6] and validate the deflection against the FEA results.

3.1 Functional validation of compliant actuator FEA model

MSAC was introduced in Ref. [6], and possible actuator configuration was introduced that utilizes a compliant lever mechanism to enable adjustable frequency and displacement properties. This actuator concept was demonstrated using finite element analysis (FEA) based on commercially-available piezoelectric elements manufactured by Thor Labs. Actuator proper-

ties could then be tuned along with control design to achieve a desired performance for an MSAC system. In this study, we realize the compliant actuator designs and compare them against the earlier FEA results to validate the FEA model predictions. The specific piezoelectric element used is the 'Piezo chips actuator' [18]; it functions only in extension (not contraction). The steady-state performance of the realized compliant actuator is shown in Fig. 5. The results confirm that the FEA model provides an accurate estimate of steady-state displacement. The FEA model, however, involves computational expense that is significant enough to motivate investigation of reduced-order compliant actuator models for control co-design (CCD) optimization studies. An alternative mathematical model is discussed below that estimates compliant actuator performance with significantly lower computational expense (specifically, few CPU clock cycles), but with slightly increased error in performance estimation.

3.2 PRBM/PRBDM for actuator design

The performance of the compliant actuator design was evaluated using a coarse-mesh FEA model. While this reduces predictive accuracy a relatively small amount compared to a fine-mesh model, it reduced computational expense significantly, which is an important consideration when using models for CCD optimization. While the actuator's steady-state performance estimation is within 9%, the computational time required to evaluate the performance of each design using the coarse-mesh FEA model was still too high for the planned early-stage MSAC CCD studies. To further mitigate computational expense, a 1R-PRBM model was developed to estimate the performance of a compliant actuator design [19]. The 1R-PRBM parameters are then used to realize a 1R-PRBDM [16] based simulation in Simulink.

The 1R-PRBM is used to determine the effort and load arms for the class 2 lever mechanism, which maximizes the deflections and minimizes the peak stress to be within the elastic limits for a material. The PRBM design approach allows analytical design performance evaluation within one or two machine cycles, enabling the quick exploration of the design space for a valid/optimal design.Using the PRBM parameters the designed compliant actuators are realized into Simulink using the PRBDM model shown in Fig. 6. The mechanical design of the compliant actuator is now reduced to determining the best independent design variables listed in Eqn. (4):

$$\Phi = [K, h, w, t, a] \tag{4}$$

The position of the joint is chosen to be at the midpoint of the compliant member; this is because the compliant structure is very small [19]. The spring stiffness (K) and maximum elastic stress ($\sigma_{\max}$) depend on the physical and material properties of the compliant structure, as defined in Eqn. (5) and Eqn. (6):

$$K = EI/h \tag{5}$$

$$\sigma_{\max} = \frac{Kw\theta_{\max}}{2I}, \tag{6}$$

where I is the area moment of inertia of the deflected member, $\theta_{\max}$ is the mechanism angular deflection, h, t, and w are the length, thickness, and width of the compliant member, and K is

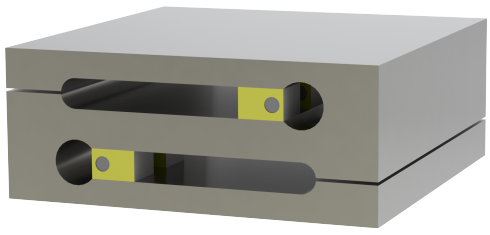

FIGURE 4: Piezoelectric actuator with compliant mechanism to amplify deflection, based on a simple class 2 lever mechanism.

(a) Actuator at rest

(b) Extended actuator

FIGURE 5: Compliant actuator steady state performance with maximum stroke

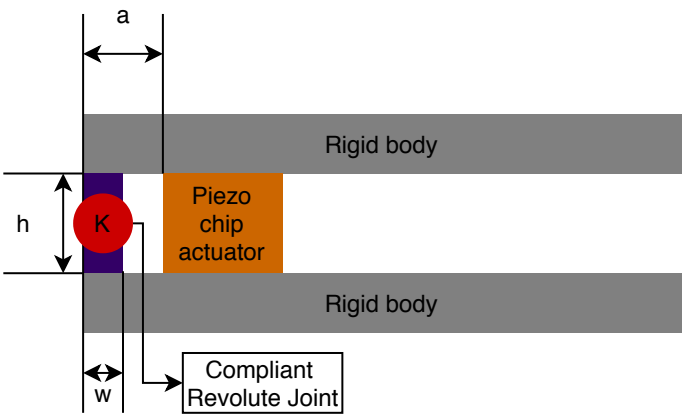

FIGURE 6: PRBDM-based compliant actuator model and independent design variables. The revolute joint is seen as red, and the compliant member is seen in purple.

Model	Hardware	FEA	PRBDM
Deflection (microns)	26.5	24	26.8
Error (%) w.r.t empirical data	0	9.5	1.13
Design performance evaluation time (secs)	-	2	0.02-0.05

TABLE 1: Hardware results vs FEA result for compliant actuator

the equivalent spring stiffness of the compliant member.

Based on this PRBDM, the performance of the compliant actuator shown in Fig. 4 can be estimated, and the comparison bewtween the model and the hardware results is presented in Table 1[1].

4 Multi-body/multi-physics simulation

Using the PRBM model, a more complex dynamical model can be realized in a multi-body physics simulation. The dynamical model relies on PRBDMs in Simulink and is realized using mechanics components available through Simscape. In this section, a pair of compliant actuators are attached to a rigid bulk mass for initial testing, referred to as stand-alone MSAC. Subsequently, a 6U CubeSat model is realized in Simulink based on PRBDMs to realize the mechanical components. The actuation force is estimated using a top-level model for the electromechanical piezo stack actuator controlled using electronic drive circuits and open-loop control trajectories.

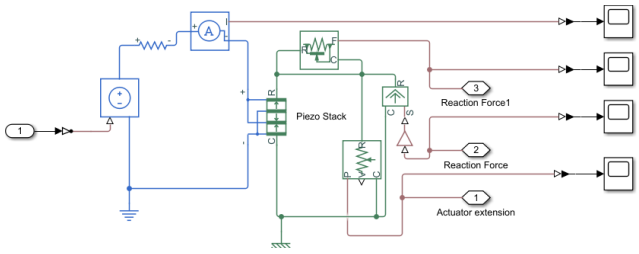

FIGURE 7: Simulink piezo stack actuator interface with Simscape Multibody components

4.1 Interfacing different physics models

The piezo-stack-actuator model is classified as an electromechanical device in Simulink. Interfacing these models with the multibody parts is a non-trivial task, and is achieved by estimating the position of a piezo stack on the application of an electrical signal, and applying a reaction force to estimate the dynamical response. An example of a piezo element that interfaces with the joints in the multibody models is illustrated in Fig. 7. The piezo stack is actuated using an ideal voltage source, and the displacements produced from the actuator are fed into the joints available from the Simscape Multibody libraries. The displacements are then fed as inputs to the joints to calculate the forces necessary to produce the displacement, and is fed back into the piezo actuation module. This reaction force is then applied with a negative unity gain on the piezo stack as a reaction force. This force feedback allows for an accurate actuator simulation based on a class 2 lever[2].

4.2 Electronics design

Realizing a multi-body Simulink model with accurate piezoelectric models allows usage of the electronics library in Simscape to realistically model the power electronics circuits that can actuate the piezoelectric actuators. Thus far, MSAC concepts have relied on the usage of half-bridge circuits that were developed for the SASA concept. These enable fast response times, but also consume more energy than other options. This is because of the probabilistic nature of mechanical noise and the wide bandwidth and phase-matching capabilities required for active noise cancellation.

Since the MSAC actuation is deterministic, the power-electronics can now be tuned for operation at a particular frequency, and reduce the power budget of the MSAC concept by one or two orders of magnitude. The realization of higher fidelity

[1]Associated code for the analytical PRBM design: https://github.com/VedantFNO/SMASIS2020/blob/master/PRBM_compliant_act_design.m

[2]Associated Simulink files for the models: https://github.com/VedantFNO/SMASIS2020/tree/master/Simulink%20files

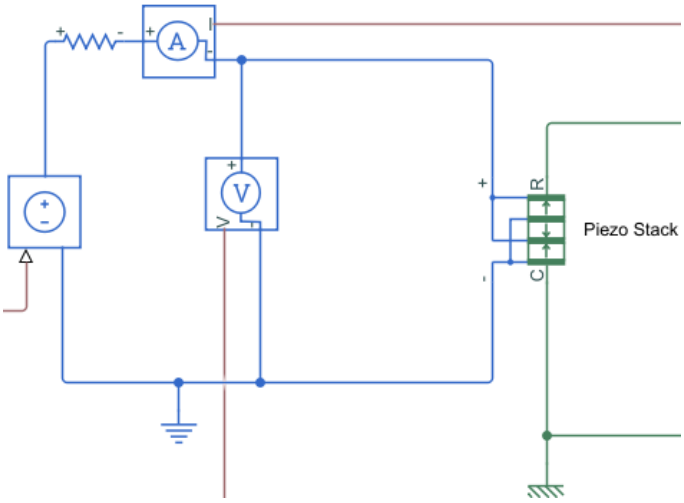

(a) Trivial electronics design

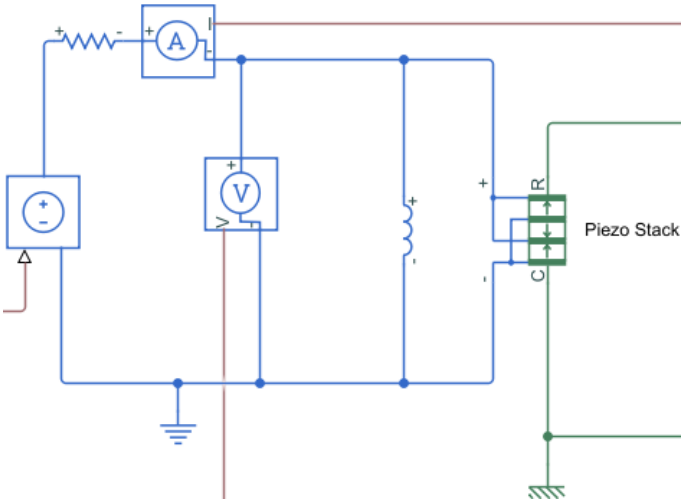

(b) Resonance electronics design

FIGURE 8: Two different circuit topologies to power piezoelectric stacks

power electronics models in the MSAC system simulation allows exploration of different circuit topologies and their impact. A tuned capacitor-inductor (LC) resonator (Fig. 8b) is one of the simplest ways to reduce the power demand of a piezoelectric element since at low frequencies the piezo element is a capacitive load. In this study, the conventional MOSFET-based design used for SASA is compared against a resonance-based circuit with respect to power consumption; the two topologies are shown in Fig. 8. As seen in Fig. 8, the voltage source is considered as an ideal Voltage source which operates in all four I-V quadrants. This simplification makes the trivial circuits in this paper more efficient than practical battery-based half-bridge circuits, more detailed electronics models will be a topic of study for subsequent studies where the gains of including power-electronics models in the CCD will be further pronounced.

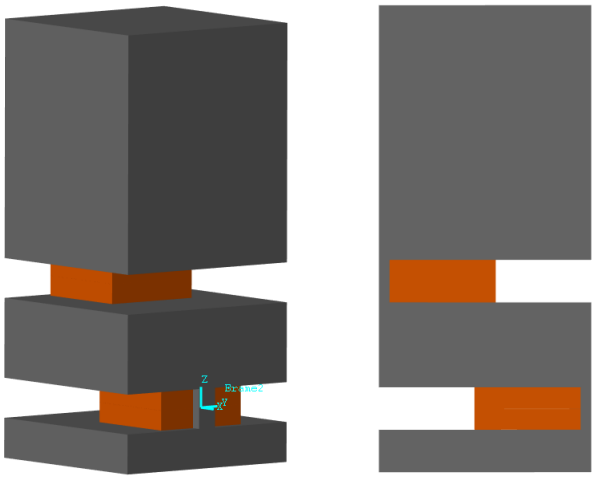

(a) Isometric view (b) Side view

FIGURE 9: Stand-alone MSAC model realized in Simulink for multi-physics simulation. The actuator is the orange monolithic element, and the compliant joint is approximated by a joint with a coordinate frame shown in teal.

5 Results and Discussions

In this section, the results from the multi-body Simulink models are presented[3]. To provide a reasonably fair comparison, the current designs are tuned for a good response for each subsystem in isolation. The associated code for mathematical models developed to enable CCD for MSAC, and multi-physics/multi-body simulations for validation, are available at Ref [20].

5.1 Stand-alone MSAC

A simple MSAC system is defined here such that it incorporates all core aspects of a related CCD problem. The MSAC actuator depicted in Fig. 6 is attached to a prismatic rigid body. The actuator, along with the rigid body, is in free space with six degrees of freedom with respect to the world frame of reference. This model allows the measurement of spacecraft body attitude slews.

The results of the Simulink model simulations for the stand-alone MSAC are provided in Table 2 , for a 10 second long simulation. Slewing performance is comparable across the two designs, but including an inductor on the electrical load side, as illustrated in Fig. 8b, reduces the power consumption by an order of magnitude. It should be noted that the system tuning was

[3]Associated graphs available on Github: https://github.com/VedantFNO/SMASIS2020/tree/master/plots

Model fidelity	Slew magnitude [mrads]	Peak slew rate [rads/sec]	Power draw [W]
Mechanical-control tuning	1.65	0.83	15.6
Mechanical-electrical control tuning	1.66	0.78	0.21

TABLE 2: Results for stand-alone MSAC simulation (time horizon :10 secs)

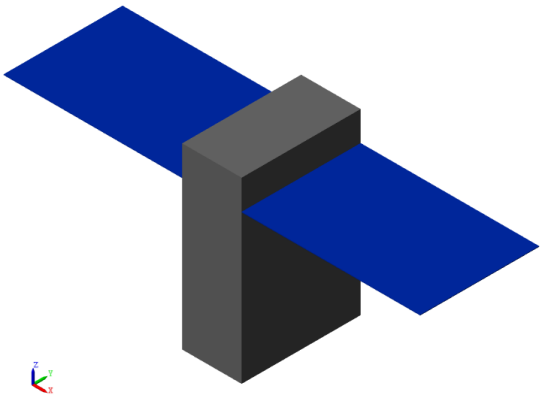

FIGURE 10: 6U CubeSat with one set of deployable MSAC panels

performed in a sequential manner, i.e., the mechanical design was tuned to maximize deflection, then the control trajectories was tuned to work close to the first natural frequency, and then finally the inductor was chosen such that the resonance of the electrical circuit matches the mechanical and control frequency. Future studies will employ CCD optimization strategies to ensure that the best possible performance for each system type is used in the comparison.

5.2 CubeSat MSAC

With the validation of the Stand-alone MSAC test, a 6U CubeSat model was realized and tested with MSAC incorporated into the CubeSat deployed panels. The attitude slews were performed about one axis, without loss of generality, and the results of the slew are shown in Fig. 11. In Fig. 11, the rotation angle plot show the attitude slew about x-axis. The angular velocity is a high-frequency periodic signal, which shows the vibration noise produced by MSAC during slews. A key thing to observe is that the signal amplitude is asymmetric about zero, showing the secular slew along the positive x-axis. Table 3 summarizes

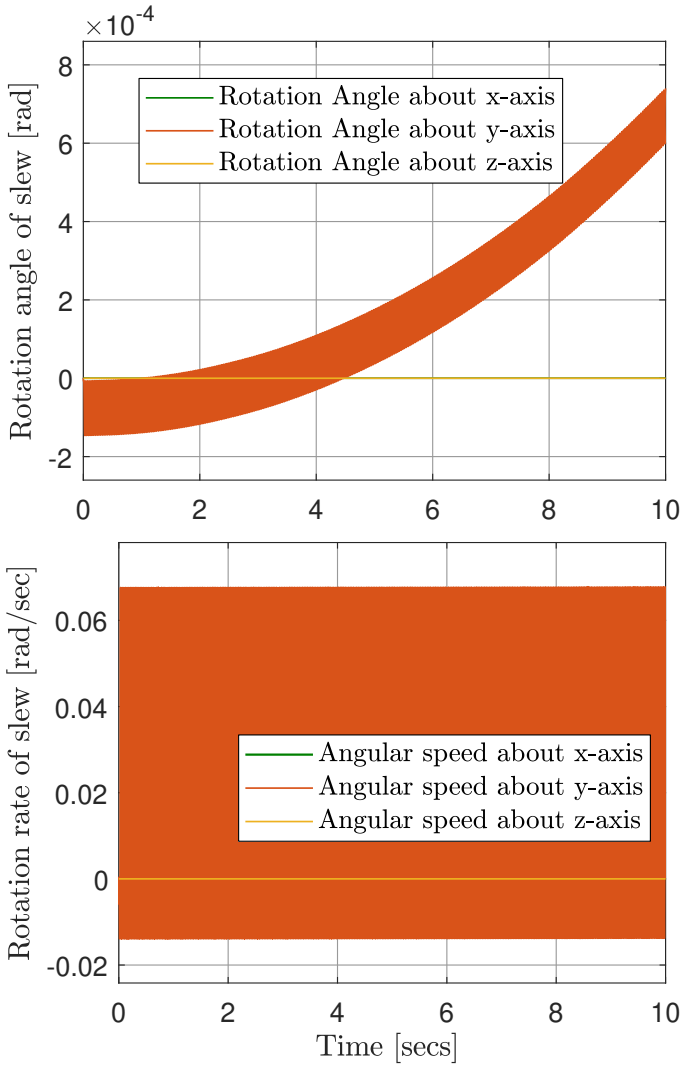

FIGURE 11: Attitude slew of the 6U CubeSat with compliant actuator designs and tuned electronics

the results from the tests for a time horizon of 10 seconds. The slews obtained from the CubeSat tests are significantly smaller than the stand-alone tests; this is because the system has not been tuned for optimal response and because the inertia ratio of a 6U satellite to a single-fold deployable panel is much larger as compared to multi-fold deployable panels. MSAC slewing response is expected to increase with an increase in the length of the deployable panels, since the moment of inertia scales with length cubed.

6 Conclusion and Future Work

In this study, mathematical models were developed to enable CCD of the MSAC system. Manual tuning was performed

Model fidelity	Slew magnitude [mrads]	Peak slew rate [mrads/sec]	Power draw [W]
Mechanical-control tuning	0.87	0.065	12
Mechanical-electrical control tuning	0.825	0.067	0.7

TABLE 3: Results for a 6U CubeSat MSAC simulation (time horizon :10 secs)

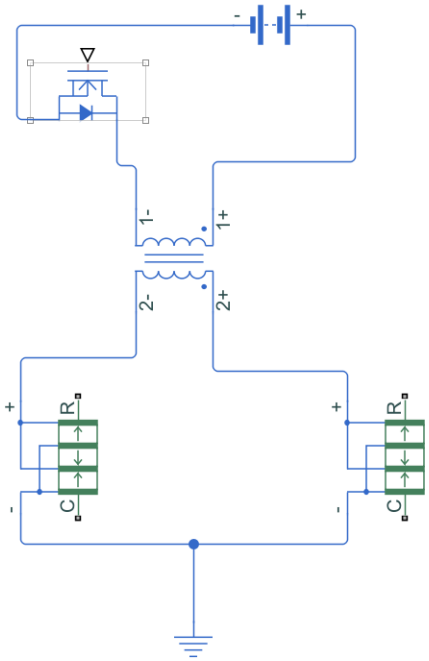

FIGURE 12: Mutual inductor based resonance circuit

in the studies presented here, but these models will be used in future CCD optimization studies. The mechanical models were approximated using a PRBM/PRBDM implemented in Simulink. The native tools of Simulink support effective control system design and have been used to perform initial informal CCD studies using the realized PRBDM. Subsequently, the value of including electrical domain design elements in the MSAC system design study was demonstrated. Specifically, this design space expansion enabled reduction of power consumption by approximately an order of magnitude. This improvement in performance is possible due to the deterministic control trajectories, and adapting electronics to capitalize on having known trajectories. The results presented in this paper were a consequence of preliminary sequential optimization/tuning of each system independent of its impact on any other subsystem.

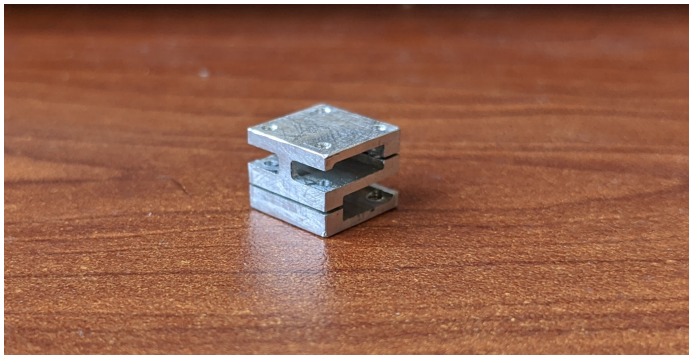

FIGURE 13: 3-DOF compliant actuator designed using PRBDM

An extension of this study will leverage the anticipated strong design coupling that exists between the mechanical, electrical, and control system domains. This extension will enable a better understanding of the tradeoffs between slew performance, power requirements, system cost, and system passive/active element complexities. This extension will utilize CCD as a tool to generate more comprehensive design data, from which a deeper fundamental understanding of MSAC design tradeoffs can be derived.

This study analyzed the electronic design of a simple LC resonator circuit; future studies could utilize this framework to analyze more complex drive circuits, such as the circuit illustrated in Fig. 12. The design in Fig. 12 powers two piezo devices and cycles the energy between them, always out of phase. The mutual inductor also allows for simpler low voltage isolated DC power supplies, which have lower power losses and volume requirements.

Some initial CCD results with different mechanisms and electronic topologies have already been realized, but their responses have not yet been validated. Once such actuator design can be seen in Fig. 13. This actuator has the same performance as the actuator realized in this study, but has two bending degrees of freedom and has a smaller form factor overall, which would enable inclusion of more actuators in a given space to improve system performance.

7 Acknowledgements

This material is based upon work partially supported by the National Science Foundation under Grant No. CMMI-1653118.

References

[1] Fields, R., Lunde, C., Wong, R., Wicker, J., Kozlowski, D., Jordan, J., Hansen, B., Muehlnikel, G., Scheel, W., Sterr, U., et al., 2009. "NFIRE-to-TerraSAR-X laser communication results: satellite pointing, disturbances, and other attributes consistent with successful performance". In Sensors and Systems for Space Applications III, Vol. 7330, International Society for Optics and Photonics, p. 73300Q.

[2] Hemmati, H., 2006. *Deep space optical communications*, Vol. 11. John Wiley & Sons.

[3] Acton, D. S., Atcheson, P. D., Cermak, M., Kingsbury, L. K., Shi, F., and Redding, D. C., 2004. "James Webb Space Telescope wavefront sensing and control algorithms". In Optical, Infrared, and Millimeter Space Telescopes, Vol. 5487, International Society for Optics and Photonics, pp. 887–897.

[4] Meza, L., Tung, F., Anandakrishnan, S., Spector, V., and Hyde, T., 2005. "Line of Sight Stabilization of James Webb Space Telescope". In 2005 AAS Guidance & Control Conference. https://ntrs.nasa.gov/archive/nasa/casi.ntrs.nasa.gov/20050139747.pdf, Accessed: 2020-06-03.

[5] McNamara, P., Vitale, S., Danzmann, K., Team, L. P. S. W., et al., 2008. "Lisa pathfinder". *Classical and Quantum Gravity,* ***25***(11), p. 114034.

[6] Vedant, and Allison, J. T., 2019. "Multifunctional Structures for Attitude Control". Vol. ASME 2019 Conference on Smart Materials, Adaptive Structures and Intelligent Systems of *Smart Materials, Adaptive Structures and Intelligent Systems*. V001T03A005.

[7] Larson, W. J., and Wertz, J. R., 1992. Spacecraft Subsystems. In: Space mission analysis and design. Tech. rep., Torrance, CA (United States); Microcosm, Inc.

[8] Harland, D. M., and Lorenz, R., 2007. *Attitude control system failures. In: Space Systems Failures disasters and rescues of satellites, rocket and space probes*. Springer Science & Business Media.

[9] Vaillon, L., and Philippe, C., 1999. "Passive and active microvibration control for very high pointing accuracy space systems". *Smart materials and structures,* ***8***(6), p. 719.

[10] Chilan, C. M., Herber, D. R., Nakka, Y. K., Chung, S.-J., Allison, J. T., Aldrich, J. B., and Alvarez-Salazar, O. S., 2017. "Co-Design of Strain-Actuated Solar Arrays for Spacecraft Precision Pointing and Jitter Reduction". *AIAA Journal,* ***55***(9), Sept., pp. 3180–3195.

[11] Herber, D. R., McDonald, J. W., Alvarez-Salazar, O. S., Krishnan, G., and Allison, J. T., 2014. "Reducing spacecraft jitter during satellite reorientation maneuvers via solar array dynamics". In 15th AIAA/ISSMO Multidisciplinary Analysis and Optimization Conference, p. 3278.

[12] Vedant, Patterson, A. E., and Allison, J. T., 2020. "Multifunctional Structures for Spacecraft Attitude Control". In 2020 AAS Guidance & Control Conference.

[13] Vedant, Ghosh, A., Alvarez-Salazar, O. S., and Allison, J. T., 2019. "Impact of Strain-Actuated Attitude Control Systems for Variant Mission Classes". In 70th International Astronautical Congress, no. C1.5.2.

[14] Coverstone-Carroll, V., and Wilkey, N., 1995. "Optimal control of a satellite-robot system using direct collocation with non-linear programming". *Acta Astronautica,* ***36***(3), pp. 149–162.

[15] "Optimal reorientation of a multibody spacecraft through joint motion using averaging theory, author=Cerven, William Todd and Coverstone, Victoria L, journal=Journal of Guidance, Control, and Dynamics, volume=24, number=4, pages=788–795, year=2001".

[16] Vedant, and Allison, J. T., 2019. "Pseudo-Rigid-Body Dynamic Models for design of compliant members". *Journal of Mechanical Design*, 12, pp. 1–22.

[17] Allison, J. T., and Herber, D. R., 2014. "Multidisciplinary Design Optimization of Dynamic Engineering Systems". *AIAA Journal,* ***52***(4), Apr., pp. 691–710.

[18] Low-Voltage Piezoelectric Chips. https://www.thorlabs.com/newgrouppage9.cfm?objectgroup_id=7563. Accessed: 2020-04-09.

[19] Howell, L. L., Magleby, S. P., and Olsen, B. M., 2013. *Handbook of compliant mechanisms*. John Wiley & Sons.

[20] MATLAB code repository: CCD of compliant actuator based MSAC. https://github.com/VedantFNO/SMASIS2020. Accessed: 2020-06-24.